

Copper Ion-Selective Fluorescent Sensor Based on the Inner Filter Effect Using a Spiropyran Derivative

Na Shao,[†] Ying Zhang,[†] SinMan Cheung,[‡] RongHua Yang,^{*†} WingHong Chan,^{*‡} Tain Mo,[‡] KeAn Li,[†] and Feng Liu[†]

College of Chemistry and Molecular Engineering, Peking University, Beijing, 100871, China, and Department of Chemistry, Hong Kong Baptist University, Kowloon Tong, Hong Kong, China

A highly selective copper(II) ion fluorescent sensor has been designed based on the UV–visible absorption of a spiropyran derivative coupled with the use of a metal porphyrin operative on the fluorescence inner filter effect. Spiroyrans, which combine the characteristics of metal binding and signal transduction, have been widely utilized in cationic ion recognition by UV–visible spectroscopy. In the present work, the viability of converting the absorption signal of the spiropyran molecule into a fluorescence signal was explored. On account of overlap of the absorption band of the spiropyran ($\lambda_{\text{abs}} = 547 \text{ nm}$) in the presence of copper ion with the Q-band of an added fluorophore, zinc meso-tetraphenylporphyrin ($\lambda_{\text{abs}} = 556 \text{ nm}$), the effective light absorbed by the porphyrin and concomitantly the emitted light intensity vary as a result of varying absorption of the spiropyran via fluorescence inner filter effect. The metal binding characteristic of the spiropyran presents an excellent selectivity for copper ion in comparison with several other heavy or transition metal ions. Since the changes in the absorbance of the absorber translate into exponential changes in fluorescence of the fluorophore, the novelty of the present device is that the analytical signal is more sensitive over that of the absorptiometry or that of the fluorometry using one single dye. To realize a practical fluorescent sensor, both the absorber and fluorophore were immobilized in a plasticized poly(vinyl chloride) membrane, and the sensing characteristics of the membrane for copper ion were investigated. The sensor is useful for measuring Cu^{2+} at concentrations ranging from 7.5×10^{-7} to $3.6 \times 10^{-5} \text{ M}$ with a detection limit of $1.5 \times 10^{-7} \text{ M}$. The sensor is chemically reversible, the fluorescence was switched off by immersing the membrane in copper ion solution and switched on by washing it with EDTA solution.

The development of optical sensing approaches for the detection of environmentally and biologically important species, such as heavy metal ions, has been an important goal in the field of

chemical sensors for several decades. Of the many different kinds of optical sensors (luminescence, absorption, reflection, etc), a fluorescence-based one is a very appealing motif for future practical applications, thanks to its intrinsic sensitivity, its straightforward application to fiber optical-based detection, and its being capable of affording high spatial resolution via microscopic imaging.^{1,2} The most direct way to construct a fluorescent sensor approach is to look for fluorescence sensory molecules instead of absorbing ones. In general, a fluorescent sensory molecule would involve the covalent linking of a receptor domain to a fluorescent fragment (i.e., the signaling unit). The two components are intramolecularly connected together such that the binding of the target analyte causes significant changes to the photophysical properties of the fluorescent fragment.^{3,4}

Spiroyrans⁵ are an important class of photo- and thermochromic compounds, which show reversible structural conversion upon the actions of external optical, chemical, and thermal stimulation.^{6–9} Irradiation with ultraviolet light causes formation of an extended π -conjugation open form (merocyanine form) by heterolytic cleavage of the C (spiro)–O bond (Scheme 1). The merocyanines may interact with their environment (i.e., solvent, matrix, etc.), leading to different photochromic responses. Several years ago,

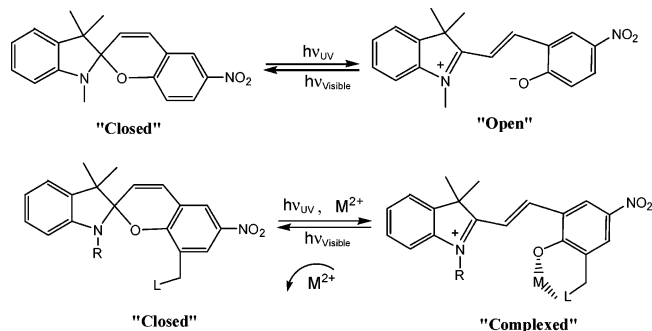
- (1) For reviews, see: (a) *Fluorescent Chemosensors for Ion and Molecule Recognition*; Czarnik, A. W., Ed.; ACS Symposium Series 538; American Chemical Society: Washington, DC, 1992. (b) *Chemosensors of Ion and Molecule Recognition*; Desvergne, J.-P., Czarnik, A. W., Eds.; NATO ASI Series C Vol. 492; Kluwer Academic Press: Dordrecht, The Netherlands, 1997. (c) Wolfbeis, O. S.; Bohmer, M.; Durkop, A.; Enderlein, L.; Gruber, M.; Klimant, I.; Krause, C.; Kurner, J.; Liebsch, G.; Lin, Z.; Oswald, B.; Wu, M. In *Fluorescence Spectroscopy, Imaging and Probes: New Tools in Chemical, Physical and Life Sciences*; Kraayenhof, R., Visser, A. J. W. G., Gerritsen, H. C., Eds.; Springer: Berlin, 2002. (d) *Handbook of Fluorescent Probes and Research Chemicals*, 9th ed.; Haugland, R. P. Ed.; Molecular Probes: Eugene, OR, 2002.
- (2) The biennial reviews on Molecular Fluorescence, Phosphorescence, and Chemiluminescence Spectrometry and Fiber-Optic Chemical Sensors and Biosensors; see, for examples: (a) Powe, A. M.; Fletcher, K. A.; St. Luce, N. N.; Lowry, M.; Neal, S.; McCarroll, M. E.; Oldham, P. B.; McGown, L. B.; Warner, I. M. *Anal. Chem.* **2004**, *76*, 4614–4634. (b) Wolfbeis, O. S. *Anal. Chem.* **2004**, *76*, 3269–3283.
- (3) For reviews of fluorescent molecule probes, see: (a) de Silva, A. P.; Nimal Gunaratne, H. Q.; Gunnlaugsson, T.; Huxley, A. J. M.; McCoy, C. P.; Rademacher, J. T.; Rice, T. E. *Chem. Rev.* **1997**, *97*, 1515–1566. (b) Valeur, B.; Leray, I. *Coord. Chem. Rev.* **2000**, *205*, 3–40. (c) Prodi, L.; Bolletta, F.; Montalti, M.; Zaccaroni, N. *Coord. Chem. Rev.* **2000**, *205*, 59–83. (d) Beer, P. D.; Gale, P. A. *Angew. Chem., Int. Ed.* **2001**, *40*, 487–516. (e) Pu, L. *Chem. Rev.* **2004**, *104*, 1687–1716. (f) Gokel, G. W.; Leevy, W. M.; Weber, M. E. *Chem. Rev.* **2004**, *104*, 2723–2750.

* To whom correspondence should be addressed. E-mail: Yangrh@pku.edu.cn; Whchan@hkbu.edu.hk. Fax: +86-10-62751708.

[†] Peking University.

[‡] Hong Kong Baptist University.

Scheme 1. Photoreversible Equilibria and Metal Complexation of Spiropyran Derivates with Divalent Metal Ions



Taylor and Phillips independently demonstrated that the negatively charged phenolic oxygen atom in the merocyanine form of a spiropyran nucleus could bind to a metal center in cooperation with other chelating function attached at the 8'-position (Scheme 1).^{10,11} During the past decade, a number of such interesting compounds have been synthesized for divalent metal ion recognition.^{12–21} More sophisticated systems, with multiple metal binding sites in the spiropyran–crown (or cryptand) ether conjugates have also been developed for alkali metal ion recognition.^{22–30} However, most of such metal binding events

reported so far have been mainly confined to UV–visible absorption spectroscopy.^{14–30} Less attention has been paid to luminescence spectroscopy due to the common susceptibility of lower quantum yields of such dyes,^{12,13} although the “signal communications” of absorption and fluorescence between a spiropyran nucleus and a fluorophore have been studied based on intermolecular energy transfer or photoinduced proton transfer.^{31,32}

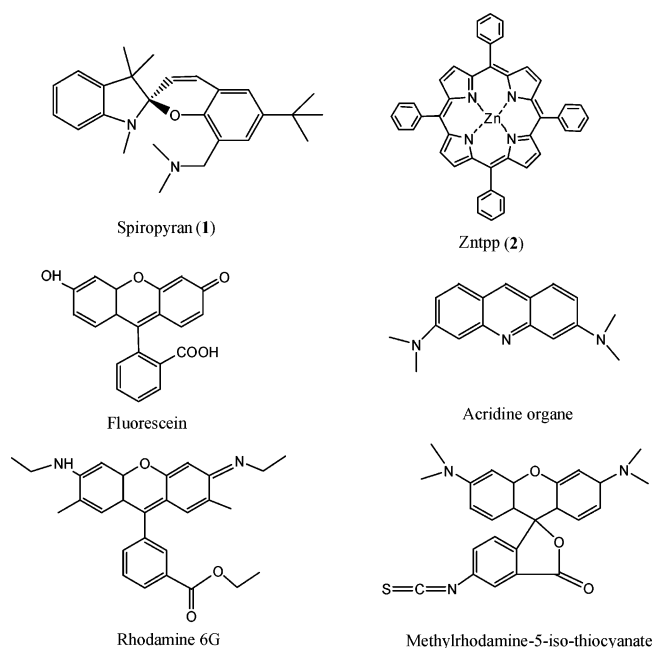
Another alternative way to convert absorbance signal into fluorescence signal without covalent linking of a chromotropic receptor and a fluorophore can be exploited by fluorescence inner filter effects (IFE). In the approach, two dyes are employed, one absorbent, the other fluorescent. If the absorption spectrum of the absorbing dye possesses a complementary overlap region with the excitation or emission spectrum of the fluorescent dye, the fluorescence emission of the fluorophore is thus modulated by the absorber.^{33–36} The IFE is a source of errors in fluorometry, but it can be useful for an optical chemical sensor by converting the analytical absorption signals into fluorescence signals.^{37–40} These sensors did not require the establishing of any covalent linking between the receptor and a fluorophore but utilize the fluorophore and the receptor as such. Moreover, since the changes in the absorbance of the absorber translate into exponential changes in fluorescence of the fluorophore, an enhanced sensitivity and decreased detection limits for the analytical method is reasonable with respect to the absorbance values alone.^{37,38}

In our preliminary experiments, we observed that the UV–visible absorption property of a newly synthesized spiropyran derivative, **1** (Chart 1), was modulated by copper ion. The metal-free state of **1** is colorless and exhibits no absorption in the visible

- (4) For selected examples of cationic ion fluorescent probes, see: (a) Nakatsuji, Y.; Kita, K.; Inoue, H.; Zhang, W.; Kida, T.; Ikeda, I. *J. Am. Chem. Soc.* **2000**, *122*, 6307–6308. (b) Watanabe, S.; Ikishima, S.; Matsuo, T.; Yoshida, K. *J. Am. Chem. Soc.* **2001**, *123*, 8402–8403. (c) Walkup, G. K.; Burdette, S. C.; Lippard, S. J.; Tsieng, R. Y. *J. Am. Chem. Soc.* **2000**, *122*, 5644–5645. (d) Chen, C. T.; Huang, W. P. *J. Am. Chem. Soc.* **2002**, *124*, 6246–6247. (e) Yang, R. H.; Chan, W. H.; Lee, A. W. M.; Xia, P. F.; Zhang, H. K.; Li, K. A. *J. Am. Chem. Soc.* **2003**, *125*, 2884–2885. (f) Ono, A.; Togashi, H. *Angew. Chem., Int. Ed.* **2004**, *43*, 4300–4302. (g) Huang, H. M.; Wang, K. M.; Tan, W. H.; An, A. L.; Huang, S. S.; Zhai, Q.; Zhou, L. J.; Jin, Y. *Angew. Chem., Int. Ed.* **2004**, *43*, 5635–5638. (h) Arunkumar, E.; Ajayaghosh, A.; Daub, J. *J. Am. Chem. Soc.* **2005**, *127*, 3156–3164.
- (5) The IUPAC nomenclature of spiropyran is 1',3',3'-dihydro-1',3',3'-trimethylspiro-[2H-1-benzopyran-2, 2'-indoline]
- (6) Fischer, E.; Hirschberg, Y. *J. Chem. Soc.* **1952**, 4522–4524.
- (7) Bertelson, R. C. In *Photochromism*; Brown, G. H.; Ed.; Wiley-Interscience: New York, 1971; pp 45–431, and references therein.
- (8) Guglielmetti, R. In *Photochromism: Molecules and Systems, Studies in Organic Chemistry*; Dürr, H., Bouas-Laurent, H. Eds.; Elsevier: Amsterdam, 1990; Chapter 8 and 23, and references therein.
- (9) Berkovic, G.; Krongauz, V.; Weiss, V. *Chem. Rev.* **2000**, *100*, 1741–1753.
- (10) Phillips, J.; Mueller, A.; Przystal, F. *J. Am. Chem. Soc.* **1965**, *87*, 4020.
- (11) Taylor, L. D.; Nicholson, J.; Davis, R. B. *Tetrahedron Lett.* **1967**, *8*, 1585–1588.
- (12) Preigh, M. J.; Lin, F. T.; Ismail, K. Z.; Weber, S. G. *J. Chem. Soc., Chem. Commun.* **1995**, 2091–2092.
- (13) Winkler, J. D.; Bowen, C. M.; Michelet, V. *J. Am. Chem. Soc.* **1998**, *120*, 3237–3242.
- (14) Chibisov, A. K.; Gorner, H. *Chem. Phys.* **1998**, *237*, 425–442.
- (15) Gorner, H.; Chibisov, A. K. *J. Chem. Soc., Faraday Trans.* **1998**, *94*, 2557–2564.
- (16) Evans, L.; Collins, G. E.; Shaffer, R. E.; Michelet, V.; Winkler, J. D. *Anal. Chem.* **1999**, *71*, 5322–5327.
- (17) Collins, G. E.; Choi, L. S.; Ewing, K. J.; Michelet, V.; Bowen, C. M.; Winkler, J. D. *Chem. Commun.* **1999**, 321–322.
- (18) Nishikiori, H.; Sasai, R.; Arai, N.; Arai, N.; Takagi, K. *Chem. Lett.* **2000**, 1142–1143.
- (19) Leautic, A.; Dupont, A.; Yu, P.; Clement, R. N. *J. Chem.* **2001**, *25*, 1297–1301.
- (20) Wojtyk, J. T. C.; Kazmaier, P. M.; Buncel, E. *Chem. Mater.* **2001**, *13*, 2547–2551.
- (21) Kopelman, R. A.; Snyder, S. M.; Frank, N. L. *J. Am. Chem. Soc.* **2003**, *125*, 13684–13685.

- (22) Inouye, M.; Ueno, M.; Kitao, T.; Tsuchiya, K. *J. Am. Chem. Soc.* **1990**, *112*, 8977–8979.
- (23) Kimura, K.; Yamashita, T.; Yokoyama, M. *J. Chem. Soc., Chem. Commun.* **1991**, 147–148.
- (24) Kimura, K.; Kaneshige, M.; Yamashita, T.; Yokoyama, M. *J. Org. Chem.* **1994**, *59*, 1251–1256.
- (25) Inouye, M.; Noguchi, Y.; Isagawa, K. *Angew. Chem., Int. Ed. Engl.* **1994**, *33*, 1163–1166.
- (26) Kimura, K.; Utsumi, T.; Teranishi, T.; Yokoyama, M.; Sakamoto, H.; Okamoto, M.; Arakawa, R.; Moriguchi, H.; Miyaji, Y. *Angew. Chem., Int. Ed. Engl.* **1997**, *36*, 2452–2454.
- (27) Filley, J.; Ibrahim, M. A.; Nimlos, M. R.; Watt, A. S.; Blake, D. M. *J. Photochem. Photobiol. A* **1998**, *117*, 193–198.
- (28) Salhin, A. M. A.; Tanaka, M.; Kamada, K.; Ando, H.; Ikeda, T.; Shibutani, Y.; Yajima, S.; Nakamura, M.; Kimura, K. *Eur. J. Org. Chem.* **2002**, 655–662.
- (29) Ahmed, S. A.; Tanaka, M.; Ando, H.; Iwamoto, H.; Kimura, K. *Eur. J. Org. Chem.* **2003**, 2437–2442.
- (30) Sakamoto, H.; Takagaki, H.; Nakamura, M.; Kimura, K. *Anal. Chem.* **2005**, *77*, 1999–2006.
- (31) (a) Bahr, J. L.; Kodis, G.; de la Garza, L.; Lin, S.; Moore, A. L.; Moore, T. A.; Gust, D. *J. Am. Chem. Soc.* **2001**, *123*, 7124–7133. (b) Guo, X. F.; Zhang, D. Q.; Zhou, Y. C.; Zhu, D. B. *J. Org. Chem.* **2003**, *68*, 5681–5687.
- (32) (a) Raymo, F. M.; Giordani, S. *J. Am. Chem. Soc.* **2002**, *124*, 2004–2007. (b) Raymo, F. M.; Giordani, S. *Org. Lett.* **2001**, *3*, 3475–3478. (c) Raymo, F. M.; Alvarado, R. J.; Giordani, S.; Cejas, M. A. *J. Am. Chem. Soc.* **2003**, *125*, 2361–2364. (d) Giordani, S.; Cejas, M. A.; Raymo, F. M. *Tetrahedron* **2004**, *60*, 10973–10981.
- (33) Parker, C. A.; Barnes, W. J. *Analyst* **1957**, *82*, 606–617.
- (34) Parker, C. A.; Tees, W. T. *Analyst* **1962**, *87*, 83–111.
- (35) Holland, J. F.; Teets, R. E.; Kelly, P. M.; Timnick, A. *Anal. Chem.* **1977**, *49*, 706–710.
- (36) Leese, R.; Wehry, E. L. *Anal. Chem.* **1978**, *50*, 1193–1197.
- (37) Yuan, P.; Walt, D. R. *Anal. Chem.* **1987**, *59*, 2391–2394.
- (38) Gabor, G.; Walt, D. R. *Anal. Chem.* **1991**, *63*, 793–796.
- (39) He, H. R.; Li, H.; Mohr, G.; Kovács B.; Werner, T.; Wolfbeis, O. S. *Anal. Chem.* **1993**, *65*, 123–127.
- (40) Yang, X. H.; Wang, K. M. Guo, C. C. *Anal. Chim. Acta* **2000**, *407*, 45–52.

Chart 1. Chemical Structures of the Absorber and Fluorophores



region; but the copper complex of **1** shows significant absorption at 547 nm. On the other hand, we observed that the Q-band absorption positions of a fluorophore, zinc meso-tetraphenylporphyrin (ZnTPP), are at 597, 556, and 518 nm. The main 556-nm band of the porphyrin overlaps nicely with the absorption band of the copper complex of **1**. Thus, the effective intensity of the excitation light beam of ZnTPP would be decreased with increasing absorbance of **1** if the two dyes coexist in a sensory device. This experimental observation encouraged us to study the possibility of detecting copper ion by ZnTPP fluorescence spectroscopy. In the present contribution, we report the IFE between ZnTPP and **1** and establish a unique determination of copper ion via the application of fluorescence sensing of the copper ion. To develop a practical fluorescent sensor, both **1** and ZnTPP were immobilized in a plasticized poly(vinyl chloride) (PVC) membrane, and the response characteristics of the sensing membrane to copper ion were investigated. In contrast to the solution-phase measurement, the polymeric membrane-based sensor possesses more favorable properties with respect to practicability. For example, the membrane-based sensor can be used routinely to achieve real-time and continuous measurements, it also allows the regeneration of the sensing reagent through simple washing procedure.

The detection of copper ion is attracting continuous attention, as copper is a significant metal pollutant due to its widespread use, but it is also an essential trace element in biological systems. Whereas copper toxicity for humans is rather low compared with other heavy metal ions, certain microorganisms are affected by submicromolar concentrations of metallic materials. Fluorescent sensing of Cu^{2+} could be utilized to clarify the physiological role of the metal in vivo as well as to monitor its concentration in the metal-contaminated sources. Although a large number of copper fluorescent sensors have been designed in the past few years,^{41–49}

there is still a need to develop a highly selective fluorescent sensing method that allows real-time monitoring of the metal ion.

EXPERIMENTAL SECTION

Materials. ZnTPP was synthesized and purified as reported previously.⁵⁰ For membrane preparation, PVC, potassium tetrakis(*p*-chlorophenyl)borate, bis(2-ethylhexyl) sebacate (BOS), and tetrahydrofuran (THF) were purchased and used. All stock solutions of metal ions were prepared from analytical grade nitrate salts and were dissolved in doubly distilled water. The work solutions of metals were obtained by series diluting the stock solutions with 0.1 M Tris-HCl buffer (pH 6.98, $I = 0.1$ (NaNO_3)). Other chemicals were of analytical reagent grade and used without further purification.

Apparatus. ^1H NMR and ^{13}C NMR were measured with an Invoa-400 (Invoa 400, 400 MHz for ^1H and 100 MHz for ^{13}C) spectrometer with tetramethylsilane as the internal standard. J values were given in hertz. Low-resolution mass spectra (MS) were obtained at 50–70 eV by fast atomic bombardment on a Finnigan MAT SSQ-710 mass spectrometer. High-resolution MS were obtained on a Q-Star Pulsar I (Applied Biosystem/PE Sciex). UV–visible measurements were performed on a Hitachi U-3010 UV/Vis spectrophotometer (Kyoto, Japan). Fluorescence spectra were conducted on a Hitachi F-4500 fluorescence spectrofluorometer with an excitation slit width of 2.5 nm and an emission slit width of 5.0 nm. Fluorescence decays were recorded using a FL920 fluorescence lifetime spectrometer. To perform the membrane measurement, a self-made flow-through measuring cell⁵¹ was used. The pH of the test solutions were measured with an electrode connected to a PHS-3C pH meter (Shanghai, China) and adjusted if necessary.

Synthesis of 1. The spiropyran derivative **1** was synthesized by a modification of the procedure reported by Phillips as outlined in Scheme 2.

(a) 5-*tert*-Butyl-2-hydroxybenzaldehyde (4). To a solution of 4-*tert*-butylphenol (**3**; 6.01 g, 40 mmol) in dry toluene (35 mL) was added SnCl_4 (1.07 g, 4.1 mmol) in dichloromethane (1.0 M, 4.1 mL). After completely mixing, Bu_3N (3.91 mL, 16.4 mmol) was added via syringe and allowed to stir for 20 min. To the reaction mixture, $(\text{CH}_2\text{O})_n$ (2.43 g, 81 mmol) was added and heated to reflux for 8 h. After cooling, the solution was poured into a separating funnel and then extracted with diethyl ether (3 \times 30 mL). The organic layer was washed with saturated NaCl solution and dried with anhydrous Na_2SO_4 . The solvent was removed, and the product was purified by silica gel chromatography using petroleum ether/ethyl acetate (9:1, v/v) as eluent to

(41) Krämer, R. *Angew. Chem., Int. Ed.* **1998**, *37*, 772–773.

(42) Grandini, P.; Mancin, F.; Tecilla, P.; Scrimin, P.; Tonellato, U. *Angew. Chem., Int. Ed.* **1999**, *38*, 3061–3064.

(43) Rurack, K.; Kollmannsberger, M.; Resch-Genger, U.; Daub, J. *J. Am. Chem. Soc.* **2000**, *122*, 968–969.

(44) Mayr, T.; Klimant, I.; Wolfbeis O. S.; Werner, T. *Anal. Chim. Acta* **2002**, *462*, 1–10.

(45) Zheng, Y. J.; Orbulescu, J.; Ji, X. J.; Andreopoulos, F. M.; Pham, S. M.; Leblanc, R. M. *J. Am. Chem. Soc.* **2003**, *125*, 2680–2686.

(46) Yang, R. H.; Zhang, Y.; Li, K. A.; Liu, F.; Chang, W. H. *Anal. Chim. Acta* **2004**, *525*, 97–103.

(47) Wu, Q. Y.; Anslyn, E. V. *J. Am. Chem. Soc.* **2004**, *126*, 14682–14683.

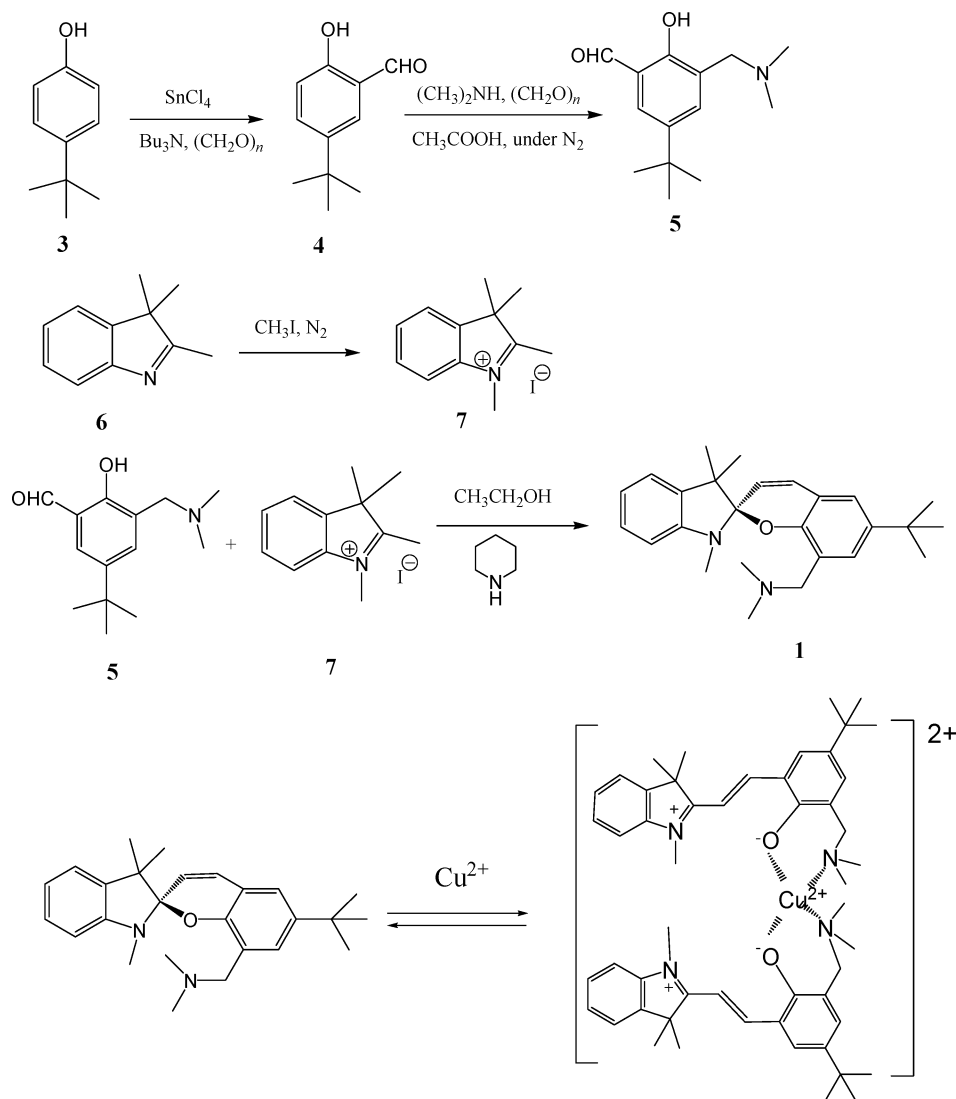
(48) Gunnlaugsson, T.; Leonard, J. P.; Murray, N. S. *Org. Lett.* **2004**, *6*, 1557–1560.

(49) Royzen, M.; Dai, Z. H.; Canary, J. W. *J. Am. Chem. Soc.* **2005**, *127*, 1612–1613.

(50) Zhang, Y.; Yang, R. H.; Li, K. A.; Liu, F. *Anal. Chem.* **2004**, *76*, 7336–7345.

(51) Wang, K. M.; Seiler, K.; Rusterholz, B.; Simon, W. *Analyst* **1992**, *117*, 57–61.

Scheme 2. Synthesis Scheme for Spiropyran 1 and the Copper Complex



give **4** as yellow oil in 85% yield. ^1H NMR (400 MHz, CDCl_3): δ 10.89(s, 1H), 9.86 (s, 1H), 7.56 (d, $J = 8.8$, 1H), 7.51 (d, $J = 2.4$, 1H), 6.91 (dd, $J = 2$, 1H), 1.32 (s, 9H). ^{13}C NMR (100 MHz, CDCl_3): δ 196.6, 159.3, 142.5, 134.5, 129.6, 119.8, 117.0, 33.9, 31.0.

(b) **5-tert-Butyl-3-[(N,N-dimethylamino)methyl]-2-hydroxybenzaldehyde (5)**.⁵² At 0 °C and under N_2 , dimethylamine (0.7 mL, 13.8 mmol) was introduced into glacial acetic acid (5.0 mL) and stirred for 15 min. $(\text{CH}_2\text{O})_n$ (0.17 g, 5.5 mmol) was added into the reaction mixture at room temperature in 15 min. After completely mixing, **4** (2.4 g, 13.5 mmol) in glacial acetic acid (2.0 mL) was injected to the reaction flask, and the resultant mixture was heated to reflux for 4 h. The reaction mixture was poured into 30 mL of water, and the pH was adjusted to slightly basic. The mixture was extracted with dichloromethane (3×30 mL). The combined organic layers were dried with anhydrous Na_2SO_4 . The solvent was removed, and the product was purified using silica gel chromatography (ethyl acetate/petroleum ether, 20:80, v/v) to give **5** in 54% yield. ^1H NMR (400 MHz, CDCl_3): δ 11.42 (s, 1H), 10.35 (s, 1H), 7.64 d, $J = 2.8$, 1H), 7.32 (d, $J = 2.4$, 1H), 3.67

(s, 2H), 2.36 (s, 6H), 1.28 (s, 9H). ^{13}C NMR (100 MHz, CDCl_3): δ 191.6, 159.5, 141.4, 132.6, 124.3, 123.4, 121.8, 61.1, 44.4, 33.8, 31.1. MS ($\text{M}^+ + 1$): 236.

(c) **N-Methyl-2, 3, 3-trimethylindolenine (7)**. Under N_2 , a mixture of 2,3,3-trimethylindolenine (**6**) (0.79 g, 5.0 mmol) and iodomethane (0.85 g, 0.61 mmol) was heated to 50 °C for 2 h. After cooling the solution to room temperature, yellow crystals were collected by filtration. The solid was washed with ethanol and diethyl ether successively. The solvent was removed under vacuum, and the residue was recrystallized from absolute ethanol to give **6** in 70% yield. ^1H NMR (400 MHz, DMSO): δ 7.92 (m, 1H), 7.83 (dd, $J = 2$, 1H), 7.62 (dd, $J = 2.8$, 2H), 2.97 (s, 3H), 2.77 (s, 3H), 1.53 (s, 6H). ^{13}C NMR (100 MHz, DMSO): δ 196.2, 142.3, 141.8, 129.5, 129.0, 123.5, 115.4, 54.2, 35.0, 21.9, 14.5.

(d) **Spiropyran 1**.⁵³ Compound **7** (0.6 g, 2.0 mmol) in absolute ethanol (30 mL) was heated to reflux. Piperidine (0.3 mL, 3.0 mmol) was added to the solution. After the resulting mixture was completely mixed, 5-tert-butyl-3-[(N,N-dimethylamino)methyl]-2-hydroxybenzaldehyde (**5**; 0.68 g, 2.0 mmol) in absolute ethanol (9.0 mL) was introduced. The mixture was refluxed for 5 h. The

(52) Larrow, J. F.; Jacobsen, E. N.; Cao, Y.; Hong, Y.; Nie, X.; Zepp, C. M. *J. Org. Chem.* **1994**, *59*, 1939–1942.

(53) Przystal, F.; Phillips, J. P. *J. Heterocycl. Chem.* **1967**, *4*, 131–132.

solvent was removed by evaporation under reduced pressure. The crude residue was purified by silica gel column chromatography using ethyl acetate/heptane (80:20, v/v) as the eluant to afford **1** as a pink solid in 89% yield.¹H NMR (400 MHz, CDCl₃): δ 7.16 (m, 2H), 7.06 (d, $J = 6.8$, 1H), 6.95 (d, $J = 2.4$, 1H), 6.81 (m, 2H), 6.46 (d, $J = 7.6$, 1H), 5.66 (d, $J = 10$, 1H), 3.20 (q, $J = 13.2$, 2H), 2.66 (s, 3H), 2.07 (s, 6H), 1.29 (s, 12H), 1.18 (s, 3H). ¹³C NMR (100 MHz, CDCl₃): δ 149.8, 142.1, 136.9, 130.0, 127.9, 127.3, 122.3, 121.3, 118.8, 118.5, 117.7, 106.5, 56.2, 51.1, 45.3, 33.9, 31.5, 28.9, 25.7, 20.4. MS(M⁺): 390.

Optode Membrane Fabrication. A typical membrane cocktail consisted of 3.6 mg (10.0 μ mol) of **1**, 0.35 mg (0.5 μ mol) of Zntpp, 50 mg of PVC, and 100 mg of BOS. These compounds were dissolved in 2.0 mL of fresh distilled THF to make a clear and homogeneous solution. A 0.1-mL aliquot of this solution was applied to the surface of a circular 25-mm-diameter quartz plate, which was mounted on a rotating (rotating frequency 600 rpm) aluminum alloy rod.⁵¹ After a spinning time of only 5 s, a thin film was coated onto the plate. From the amount of materials employed, we estimate the thickness of the membrane to be 2–4 μ m.

Optical Measurements. The absorption and fluorescence titrations of metal ions in ethanol solution were run by directly adding small aliquots (typically 20 μ L) of the metal stock solutions to 1.5 mL of the ethanol solution containing 5.0×10^{-5} M **1** and 2.5×10^{-6} M Zntpp in a quartz sample cuvette (1 cm \times 1 cm). After being mixed thoroughly and allowed to equilibrate for 5 min, the absorption or fluorescence spectra were then recorded at room temperature.

To assess the fluorescence responses of the optode membrane to copper ion, the quartz plate with sensing membrane was first fitted onto the front side of the measuring cell. A 25-mm-diameter black PVC plate without sensing membrane was then fitted onto the other side to complete the cell. The cell was introduced into the spectrofluorometer at the appropriate position⁵⁴ to measure the fluorescence emission without interference from the excitation source. About 2.0 mL of sample solution was introduced, and the fluorescence spectra of the optode membrane were recorded with an excitation wavelength of 556 nm and an emission wavelength of 603 nm. Before each measurement, the membrane was conditioned in plain buffer until the fluorescence intensity was stabilized.

RESULTS AND DISCUSSION

Choices of Absorber and Fluorophore. As the starting point, the performance of IFE requires the presence of two dyes, one acting as analyte-sensitive absorber and the other as the analyte-independent fluorophore whose the excitation or emission intensity is modulated by varying the absorption of the absorber. The requisite copper-sensing absorber, spirospyran **1**, was synthesized in a three-step convergent sequence shown in Scheme 2. To achieve strong and highly specific binding to metal ion, the ion receptor domain of the spirospyran nucleus was formed by introducing a dimethylaminomethyl moiety in the 8'-position of the molecule via the Mannich reaction. The bidentate N,O-chelating binding site present in the molecule would generate

great affinity toward the d- and f-elements.^{55,56} Additionally, as a practical sensory material, the metal binding interaction of the spirospyran should be chemically reversible rather than photochromically reversible. It was demonstrated that, for a given medium, the position of equilibrium of the closed form and open form of a spirospyran nucleus usually depends on the nature of the substituent group in 6'-position. A strong electron-withdrawing group in 6'-position produces a stable open form, while an electron-donating group in the position leads to a more photostationary closed state.^{11,57,58} Therefore, a *tert*-butyl group was introduced in the 6'-position, superseding the nitro group in the position to obtain a stable optical signal without photochromic behaviors triggered by irradiating with ultraviolet light or visible light. As an additional merit in the sensor design, the introducing of an alkylated chain in the molecular skeleton ensures its high hydrophobicity of the material, which meets the basic condition for a component in a polymeric film.

To exploit the IFE for fluorescence response to the absorption change of **1**, a set of fluorophores were then tested. Although many organic fluorescent dyes such as fluorescein ($\lambda_{\text{ex}}/\lambda_{\text{em}} = 496/520$ nm), acridine orange ($\lambda_{\text{ex}}/\lambda_{\text{em}} = 490/530$ nm), rhodamine 6G ($\lambda_{\text{ex}}/\lambda_{\text{em}} = 530/590$ nm), and methylrhodamine-5-iso-thiocyanate ($\lambda_{\text{ex}}/\lambda_{\text{em}} = 541/572$ nm) exhibit an excellent excitation or emission spectrum overlapping with the absorption maximum of the copper complex of **1**, they cannot function as a fluorescent indicator in the present system, since the fluorescence of such dyes is seriously quenched by copper ion. Thus, it is impractical to use any of them to signal fluorescently the metal binding event via IFE. To meet our need, we decided to use a metallorganic fluorophore, Zntpp, as the fluorescent reporter. Although the maximal emission position of Zntpp locates at 603 nm, the Q-band absorption positions of the porphyrin are at 597, 556, and 518 nm, the main 556-nm band overlaps well with the absorption band of the copper complex of **1**. Therefore, if the two dyes are present simultaneously in this approach, the effective intensity of the excitation light beam of Zntpp at 556 nm will be decreased with increasing absorbance of **1** as a result in response to increasing copper ion concentration. Further, we selected Zntpp as the fluorophore because of its fluorescence feature free from the influence of external factors such as pH, metal ions, and anions (see below).

Binding Interactions of **1 and Metal Ions.** Prior to application in fluorescence sensing of copper ion, the binding interaction of **1** with divalent metal ions was first studied by UV-visible spectroscopy. Figure 1 shows the absorption spectra of **1** in ethanol. The free state of **1** is colorless (5.0×10^{-5} M) and the absorption spectrum displays an absorption maximum at 314 nm. No significant absorption is observed in the visible region, which indicates the nearly complete absence of the merocyanine component. Figure 1 also shows the absorption spectral changes of **1** in the presence of 5.0×10^{-5} M Hg²⁺, Cd²⁺, Zn²⁺, and Cu²⁺, respectively. The absorption spectrum of **1** was hardly influenced

(54) Yang, R. H.; Wang, K. M.; Xiao, D.; Yang, X. H.; Li, H. M. *Anal. Chim. Acta* **2000**, *404*, 205–211.

(55) Barthram, A. M.; Ward, M. D.; Gessi, A.; Armaroli, N.; Flamigni, F.; Barigelletti, F. *J. New Chem.* **1998**, 913–917.

(56) Tong, H.; Wang, L. X.; Ting, X. B.; Wang, F. *Macromolecules* **2002**, *35*, 7169–7171.

(57) Keum, S.-R.; Lee, K.-B.; Kazmaier, P. M.; Buncl, E. *Tetrahedron Lett.* **1994**, *35*, 1015–1018.

(58) Swansburg, S.; Bucel, E.; Lemieux, R. P. *J. Am. Chem. Soc.* **2000**, *122*, 6594–6600.

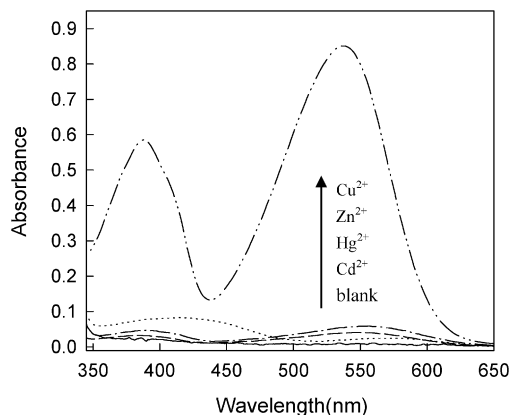


Figure 1. UV-visible absorption spectra of **1** (5.0×10^{-5} M) in ethanol solution in the absence and presence of 5.0×10^{-5} M Cd^{2+} , Hg^{2+} , Zn^{2+} , and Cu^{2+} , respectively.

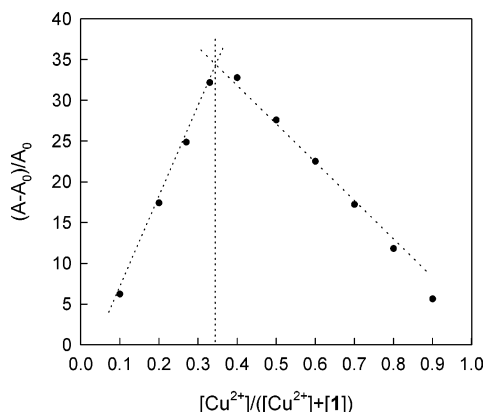


Figure 2. Job plot for determining the stoichiometry of **1** and Cu^{2+} . The total concentration of **1** and copper was 1.0×10^{-4} M. Molar fraction was given by $[\text{Cu}^{2+}]/([\text{Cu}^{2+}] + [\mathbf{1}])$.

by addition of Hg^{2+} or Cd^{2+} , separately, while a small enhancement in the absorbance was observed upon the addition of Zn^{2+} . In contrast, when Cu^{2+} was added to the ethanol solution of **1**, a pink solution appeared with a strong absorption peak at 547 nm. The absorbance of **1** at 547 nm is increased to 77.2-fold that of the original value by Cu^{2+} (5.0×10^{-5} M), but it is only 2.34-fold by Cd^{2+} , 4.16-fold by Hg^{2+} , and 7.84-fold by Zn^{2+} .

UV-visible spectroscopy was followed as aliquots of copper(II) nitrate were added to the solutions of **1**. Dramatic increase in the absorbance of **1** at 547 nm was evident with increasing concentration of copper ion up to ~ 0.5 equiv relative to the host concentration. To determine the stoichiometry of the copper–ligand complex, Job's method for the absorbance was applied, keeping the sum of the initial concentration of copper ion and **1** at 1.0×10^{-4} M, and the molar ratio of copper ion changing from 0 to 1.^{59,4h} The absorbances of **1** in the absence (A_0) and presence (A) of copper ion were determined, respectively. A plot of $(A - A_0)/A_0$ versus the molar fraction of copper ion is provided in Figure 2. It shows that the $(A - A_0)/A_0$ value goes through a maximum at a molar fraction of ~ 0.33 , indicating a 1:2 stoichiometry of the Cu^{2+} to **1** in the complex.

The association constant can be determined from the absorption titration data. If a 1:2 metal–ligand complex is formed

between Cu^{2+} and **1**, one can describe the equilibrium as follows:



where SP and $\text{Cu}(\text{SP})_2$ denotes **1** and its copper complex, respectively. The corresponding association constant, K , can be expressed as follows:

$$K = \frac{[\text{Cu}(\text{SP})_2]}{[\text{SP}]^2[\text{Cu}^{2+}]} \quad (2)$$

According to the derivation reported elsewhere,⁶⁰ a response function for Cu^{2+} is given below following the mass law:

$$\frac{\alpha^2}{1 - \alpha} = \frac{1}{2KC_T[\text{Cu}^{2+}]} \quad (3)$$

where C_T denotes the total concentration of **1** in the system. The α term in eq 3 can be defined as the ratio of the concentration of uncomplexed **1** to the total concentration of **1** present in the system.

$$\alpha = [\text{C}]/C_T \quad (4)$$

α can be determined from the absorbance changes in the presence of different concentrations of Cu^{2+} :

$$\alpha = (A - A_0)/(A_1 - A_0) \quad (5)$$

where A_1 and A_0 are the limiting absorbance values for $\alpha = 1$ (in the absence of Cu^{2+}) and $\alpha = 0$ (**1** is completely complexed with Cu^{2+}), respectively. The term α can also be named relative absorption signal. It is apparent from eq 3 that the response parameter (α) has a distinct functional relationship with the concentration of copper ion and the association constant, K . Equation 3 provides the basis for the determination of K value. The experimental data were fitted to eq 3 by adjusting the K value. Figure 3 shows the fitted curve to incorporate the experimental data for copper ion, which refers to $\log K = 6.8$.

To study the binding affinity of **1** to other divalent metal ions, **1** was subjected to different concentrations of alkaline-earth and heavy metals, separately (see Supporting Information). Additional spectral properties of the metal complexes of **1** are summarized in Table 1. The very large extinction coefficient of the copper complex can contribute to the susceptibleness of the fully occupied d-orbit of Cu^{2+} . The response selectivity factors of **1** for different metal ions were evaluated by comparing the binding affinity of **1** to metal ion and the absorption enhancement of **1** by metal ion ($K\epsilon$),⁶¹ where K is the association constant of **1** with metal ion and ϵ is the extinction coefficient of the metal complex. The response to copper ion was used as the standard. On the basis of

(60) Yang, R. H.; Li, K. A.; Wang, K. M.; Zhao, F. L.; Li, N.; Liu, F. *Anal. Chem.* **2003**, *75*, 612–621.

(61) Zhao, J. Z.; Fyles, T. M.; James, T. D. *Angew. Chem., Int. Ed.* **2004**, *43*, 3461–3464.

(59) Job, P. *Ann. Chim.* **1928**, *9*, 113–116.

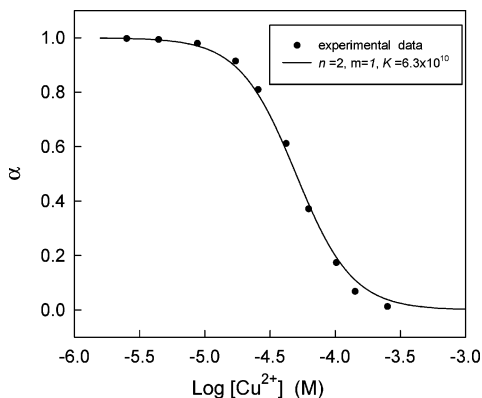


Figure 3. Response parameter (α) as a function of logarithm of Cu^{2+} concentration at pH 6.98. The curve fitting the experimental points (●) was calculated from eq 3.

Table 1. Absorption Properties of 1 and Its Metal Complexes in the Visible Region, Association Constants, K , and Response Selectivity of 1 to Metal Ions

species	λ_{max} (nm)	ϵ , 10^3 ($\text{M}^{-1}\text{cm}^{-1}$)	K (M^{-2})	response selectivity ^a
1	552	0.44		
1 + Cu^{2+}	547	31.2	6.31×10^6	1
1 + Mg^{2+}	560	0.50	3.42×10^2	9.66×10^{-7}
1 + Ca^{2+}	554	0.57	2.65×10^2	8.53×10^{-7}
1 + Cd^{2+}	560	0.87	1.12×10^4	5.50×10^{-4}
1 + Co^{2+}	552	2.85	3.02×10^5	4.86×10^{-4}
1 + Ni^{2+}	572	0.69	5.36×10^4	2.09×10^{-6}
1 + Zn^{2+}	574	3.04	6.67×10^4	1.15×10^{-4}
1 + Hg^{2+}	556	1.62	1.90×10^3	1.74×10^{-5}
1 + Mn^{2+}	562	0.53	8.56×10^2	2.56×10^{-6}
1 + Pb^{2+}	554	0.72	1.08×10^3	4.39×10^{-6}

^a Response selectivity, $(K_i\epsilon_i) / (K_{\text{Cu}}\epsilon_{\text{Cu}})$.

the spectroscopic data in Table 1, one can easily recognize that remarkably high selectivity of **1** for Cu^{2+} is realized.

A series of 6'-nitro substituent spiropyran derivatives have been widely used to investigate the photoinduced metal binding interaction.⁹ The 6'-nitro group withdraws electron density from the phenolate oxygen, which decreases the density of phenolate oxygen and thereby facilitates formation of the merocyanine form to bind almost all divalent metal ions. On the contrary, the 6'-*tert*-butyl group (electron-donating group) in **1** tends to produce a photostationary spiropyran state with a negligible merocyanine component, which will reduce its metal binding ability. This seemingly *nonactivated* spiropyran has rather limited use in photochromic application, but it could be exploited as a practical sensor with respect to its metal binding selectivity and optical signal stability. We reasoned that the strong binding affinity of **1** toward Cu^{2+} over other divalent metal ions may contribute to the particularly high thermodynamic affinity of copper for N,O-chelate ligands and the fast metal-to-ligand binding kinetics.^{41,13}

In view of photoreversible structural conversion of the merocyanine metal complex, the real-time records of the metalation degree of **1** were carried out in ethanol using the 547-nm band absorption as a function of time. As shown in Figure 4, the formation of the metal complex proceeds rapidly at first, followed by more gradual increase in the absorption. In addition, the reaction time increases with Cu^{2+} concentrations. Figure 4 also

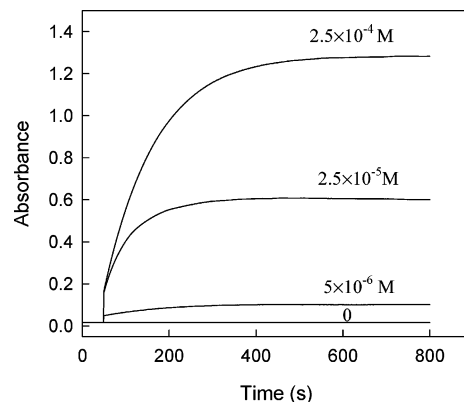


Figure 4. Kinetics of **1** reaction with different concentrations of Cu^{2+} . Absorbance was recorded at 547 nm in 5.0×10^{-5} M **1** in ethanol solution.

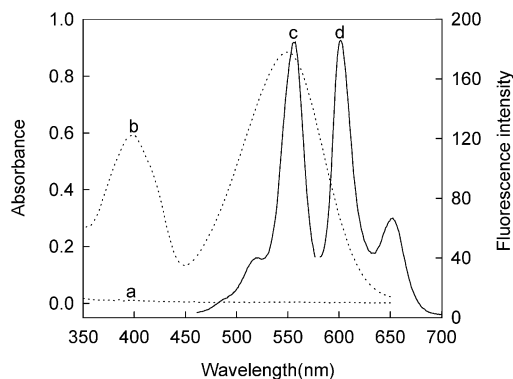


Figure 5. Absorption spectra of **1** in the absence (a) and presence of 5.0×10^{-5} M copper ion (b), and fluorescence excitation ($\lambda_{\text{em}} = 603$ nm (c)) and emission spectra ($\lambda_{\text{ex}} = 556$ nm (d)) of Zntpp.

shows the merocyanine copper complex is reasonably photostable. Irradiating the colored solution with visible light did not liberate metal ion with regeneration change of the absorbance. We envisioned that the 6-*tert*-butylphenolate merocyanine was a better ligand for the metal ion than 6-nitrophenolate formation. The 6-nitro group withdraws electron density from the phenolate oxygen, decreasing the density of the ligand and thereby facilitating reversible binding.¹⁴ The liberation of copper ion from the complexed solution could be readily achieved by addition of EDTA to the complexed solution, demonstrating that the binding is readily chemically reversible.

Fluorescence Inner Filter Effect between 1 and Zntpp in the Presence of Copper Ion. Figure 5 shows the absorption spectra of **1** and the fluorescence spectra of Zntpp at different experimental conditions. In the present approach, the states of the metal-free and metal-bound of **1** show different absorption behaviors, the copper complex of **1** is highly absorbing, which absorbs in the visible region of 450–600 nm, but the metal-free form is not as shown in curves a and b. The curves c and d are the fluorescence excitation and emission spectra of Zntpp. The excitation maximum of Zntpp in the Q-band region is at 556 nm, which has an excellent overlap with the absorption spectrum of the copper complex of **1**. The two bands of the emission spectrum at 603 and 654 nm are assigned to 0–0 and 1–0 vibronic transitions of Zntpp.^{62,63} Since the absorbance of both dyes follows the Beer–Lambert law, the relative quantities of the light absorbed at 556 nm by each of them is determined by the ratio of the

extinction coefficients at that wavelength. Thus, it is possible that the efficient light absorbed at 556 nm by Zntpp and, concomitantly, the emitted light intensity will be reduced with increasing absorbance of **1** in response to increasing copper ion concentration. Fluorescence spectroscopy was followed as aliquots of copper(II) nitrate were added to the ethanol solutions containing **1** and Zntpp. As expected from the original design, both the fluorescence excitation and emission intensities of Zntpp remarkably decrease by adding increasing concentrations of copper ion to the **1** + Zntpp ethanol solution without changes of the spectral feature (see Supporting Information). This spectral change constitutes the basis for the fluorescent detection of copper ion based on IFE.

The observed decrease in fluorescence intensity of the Zntpp may also be attributed to the possibility that copper ion directly quenches the Zntpp fluorescence. To clarify this issue, the effect of copper ion on the fluorescence spectra of Zntpp in the absence of **1** was also studied. The fluorescence signal of Zntpp without **1** hardly changes when copper ion concentration increases, which demonstrates that the absorber, **1**, is the key player to regulate the fluorescence intensity of the fluorophore, Zntpp.

Excited-state fluorescence energy transfer has been studied between covalently linked spiropyran and fluorophore.³¹ To test whether there is energy transfer between **1** and Zntpp in the present approach, decay curve measurements of **1** + Zntpp in ethanol were performed using a multichannel analyzer operating with 512 channels at 20 °C.⁶⁴ In the absence of copper ion, global analysis of the resulting data as a single-exponential decay gave a satisfactory fit ($\chi^2 = 1.218$) with a lifetime of 2.18 ns, which is nearly a lifetime for Zntpp in ethanol,^{63,65,66} indicating that **1** has no significant effect on the lifetime of the porphyrin. When copper ion was added to the solution of **1** and Zntpp, the decay curve was slightly complicated and could be fitted as monoexponential decay with two lifetimes ($\chi^2 = 1.194$). The lifetime of the major component (97.3%) was 2.07 ns, while that of the other component (2.7%) was 5.7 ns. The almost no lifetime change of the major component indicates that there is no significant excited-state interaction between **1** and Zntpp in the presence of copper, further demonstrating that the fluorescence change of Zntpp by copper is due to the simple absorption of the excitation light by the absorber.

Fluorescent Sensing of Copper Ion. The fluorescence response of **1** + Zntpp to copper ion is strongly dependent on the relative amount of the fluorophore and absorber. This can be seen in the variation of the response characteristics (working range and response sensitivity) due to the different amount ratios of fluorophore and absorber. In Figure 6, the fluorescence quenching efficiencies (F_0/F) of Zntpp by copper ion for three composition ratios are plotted as functions of the concentration of Cu^{2+} at pH 6.98, where F_0 and F are the fluorescence intensities

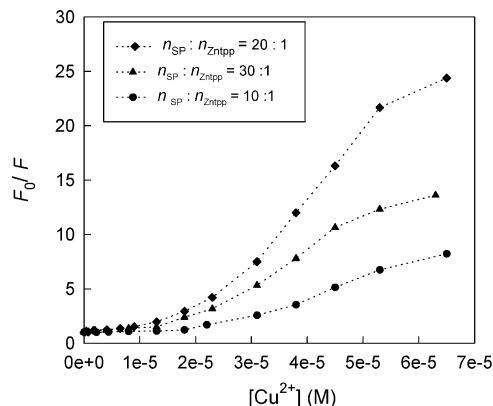


Figure 6. Effects of different composition ratios of **1** and Zntpp on the fluorescence responses to Cu^{2+} . The excitation was at 556 nm, and emission was recorded at 603 nm.

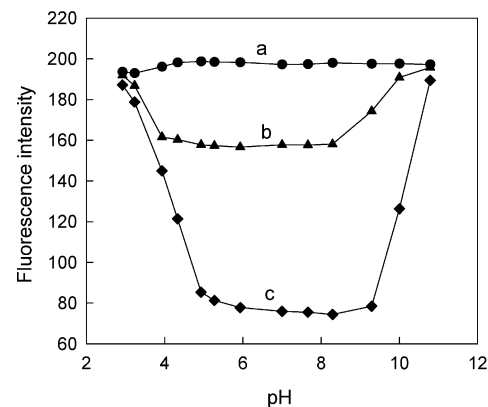


Figure 7. Fluorescence intensity–pH profiles for titrations of the ethanol solution containing 5.0×10^{-5} M **1** and 2.5×10^{-6} M Zntpp in the absence (a) and presence of 4.5×10^{-6} M (b) and 1.8×10^{-5} M (c) copper ion. The excitation was at 556 nm, and emission was recorded at 603 nm.

of Zntpp at $\lambda_{\text{ex/em}} = 556/603$ nm in the absence and presence of Cu^{2+} . Obviously, when the molar ratio of **1** to Zntpp reaches 20:1, the best response emerged in terms of the sensitivity and efficient detection range for Cu^{2+} . Lower concentration of Zntpp in the system results in the weak blank fluorescence signal value, which will reduce the dynamic working range of the measurement; while at relatively higher fluorophore concentration, the fluorescence of Zntpp could not be quenched completely even if a high concentration of copper ion was added to the solution. The response slope, dynamic working range, and detection limit of the system could be tuned by controlling the relative amounts of the absorber and fluorophore. This is one of the advantages that the IFE method has over the fluorometry based on a single fluorophore. The flexibility of component controlling allows us to monitor the metal ion concentration with appropriate adjustment of the amount of the absorber, so that the sample response falls within the most sensitive response region.

The ligation interaction of **1** with copper ion was influenced by the acidity of the medium. Figure 7 depicts the pH dependence of fluorescence changes of Zntpp in the absence and presence of copper ion. The titration experiments were carried out by adding standard NaOH or H_2SO_4 solution to a solution containing 5.0×10^{-5} M **1**, 2.5×10^{-6} M Zntpp as well as copper ion. It is obvious that the fluorescence signal of Zntpp in the absence of copper

(62) Gust, D.; Moore, T. A.; Moore, A. L.; Macpherson, A. N.; Lopez, A.; DeGraziano, J. M.; Gouni, I.; Bittersmann, E.; Seely, G. R.; Ronald, F. G.; Ma, X. C.; Demanche, L. J.; Hung, S.-C.; Luttrull, D. K.; Lee, S.-J.; Kerrigan, P. K. *J. Am. Chem. Soc.* **1993**, *115*, 11141–11152.

(63) Yu, H.-Z.; Baskin, J. S.; Zewail, A. H. *J. Phys. Chem. A* **2002**, *106*, 9845–9854.

(64) The decay curves are shown in Supporting Information.

(65) Cho, H. S.; Rhee, H.; Song, J. K.; Min, C.-K.; Takase, M.; Aratani, N.; Cho, S.; Osuka, A.; Joo, T.; Kim, D. *J. Am. Chem. Soc.* **2003**, *125*, 5849–5860.

(66) Mataga, N.; Shibata, Y.; Chosrowjan, H.; Yoshida, N.; Osuka, A. *J. Phys. Chem. B* **2000**, *104*, 4001–4003.

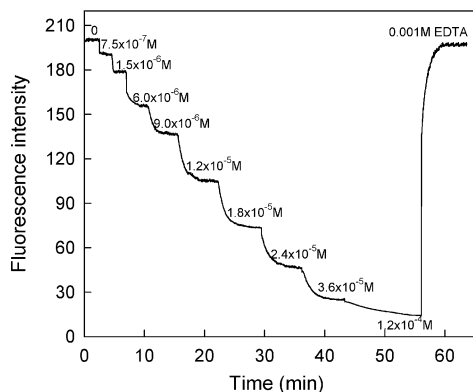


Figure 8. Time history of the sensing membrane responses to different concentrations of Cu^{2+} . Fluorescence intensity was recorded at 603 nm with an excitation wavelength of 556 nm.

ion is independent of pH in the range of 3.0–11.0 (curve a). Curves b and c show the pH dependences of the Zntpp fluorescence response to 4.5×10^{-6} and 1.8×10^{-5} M copper ion, respectively. The efficient pH range for copper ion detection is 5.0–9.0. At a pH value below 5.0, **1** converted to its protonated merocyanine form (HME^+), which reduces its ligation with copper ion; while at relatively higher pH, copper ion may be complexed by OH^- , which in turn reduces its complex with **1**.

With the optimum conditions (pH 6.98, $n_{\text{Zntpp}}:n_{\text{SP}} = 1:20$), the sensing characteristics of a PVC membrane containing **1** and Zntpp were studied. Figure 8 shows the typical response of the sensing membrane to Cu^{2+} , as obtained after equilibration with Tris-HCl buffer solutions containing different concentrations of Cu^{2+} . The fluorescence intensity was recorded after equilibration with different concentrations of Cu^{2+} with excitation at 556 nm and emission at 603 nm. The values of the fluorescence intensity of the optode membrane decrease considerably as the concentration of copper ion increases. This illustrates that the optode membrane can be used for assay of copper ion in aqueous sample solution. The optode membrane exhibited the highest sensitivity to Cu^{2+} in the 7.5×10^{-7} – 3.6×10^{-5} M range. The limit of detection, which was determined by alternately exposing the optode membrane 3 times to plain buffer and low concentration of Cu^{2+} and calculating the Cu^{2+} concentration corresponding to signal changes that are 6 times the standard deviation of the plain buffer signal, was found to be 1.5×10^{-7} M.

The reproducibility and reversibility of the optode membrane were evaluated by repetitively exposing it to 1.2×10^{-5} M copper solution and Tris-HCl buffer solution (pH 6.98). The mean fluorescence intensity values with their confidence intervals were found to be 107.63 ± 2.86 ($n = 5$, 1.2×10^{-5} M copper ion) and 197.7 ± 3.41 ($n = 5$, Tris-HCl buffer solution). The response time of the sensor depends on the thickness of the membrane, the flow rate of the sample solution, and the change of the concentration of copper ion. When the thickness of the membrane reaches the order of millimeters, there was no significant fluorescence response observed even when the membrane was immersed in copper ion solution for several hours. To prepare very thin membranes, the spin-on technique was used, which allows the production of very thin, homogeneous, and reproducible PVC-based membranes. The forward response time (going from lower to higher copper ion concentration), t_{95} (time needed for 95% of

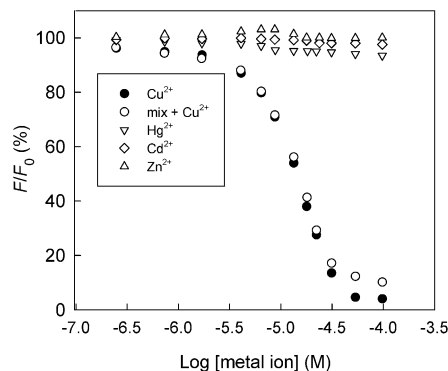


Figure 9. Fluorescence quenching of Zntpp by increasing concentrations of Cd^{2+} , Hg^{2+} , Zn^{2+} , and Cu^{2+} , separately, as well as a mixture of 1.0×10^{-3} M Mg^{2+} and Ca^{2+} and 5.0×10^{-5} M Hg^{2+} , Cd^{2+} , and Zn^{2+} with increasing concentrations of Cu^{2+} . The ordinate shows the fluorescence quenching (F/F_0). The excitation was at 556 nm, and emission was recorded at 603 nm.

total signal change to occur), was within 6 min. The liberation of copper ion from the membrane could be achieved by contacting it with Tris-HCl buffer containing 0.001 M EDTA, whereas the time for the reverse response was in the range of 3–5 min over the entire concentration range. The response time of such an optode membrane is mainly governed by the diffusion process in the bulk of the membrane and particularly the rate of complex formation. Shaking the cell can shorten the response time by ~ 2 min. Dynamic flow of the sample solution can also shorten the response time.

From the fluorescence signal values of 1.2×10^{-5} M copper ion taken every 15 min over a period of 6 h, a mean fluorescence intensity value of 105.76 and a standard deviation of 3.93 were obtained. The stability of the sensor at short times is reasonable. The optode membrane is mainly subject to the photochemical reaction and the leaching of **1** on which the lifetime of the optode depends. The fluorescence response value of the optode membrane decreased $\sim 8\%$ after a continuous 100 measurements. In addition, the leaching of plasticizer also affects the response time. It would take 3–5-fold more time to reach t_{95} than that of the freshly prepared membrane if the membrane is stored in buffer solution for longer than two weeks. Nevertheless, the lifetime of the optode membrane is acceptable for analytical application.

The fluorescence response of the sensor to copper ion presents excellent selectivity in comparison with other heavy metal ions. Zn^{2+} , Hg^{2+} , and Co^{2+} showed relatively weak effects on the Zntpp fluorescence, while Mg^{2+} , Ca^{2+} , Mn^{2+} , Pb^{2+} , and Ni^{2+} could not induce any change in the Zntpp fluorescence even with a high concentration of the metal ion present in the sample solution. To explore further the utility of the membrane as a copper-selective fluorescent sensor, competition experiments were also conducted in which the membrane was first immersed in a mixture of other metal ions, and Cu^{2+} was then added to the mixture with increasing concentrations. Figure 9 illustrates the changes of Zntpp fluorescence intensity upon additions of different concentrations metal ions as well as a mixture containing 1.0×10^{-3} M Mg^{2+} and Ca^{2+} and 5.0×10^{-5} M Hg^{2+} , Cd^{2+} , and Zn^{2+} with increasing amounts of copper ion. No significant variations in the fluorescence intensity were found by comparison with those without other metal ions rather than Cu^{2+} .

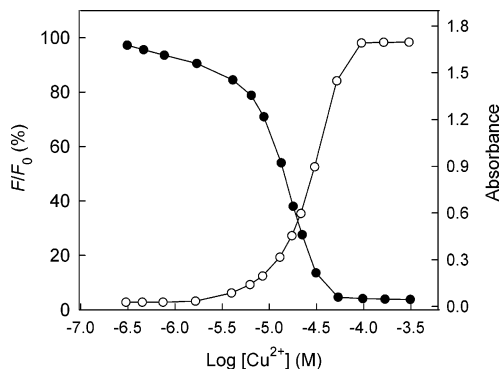


Figure 10. Comparison of absorptiometric and fluorometric techniques for copper ion detection.

Comparison of Fluorometric and Absorptiometric Techniques. To compare the analytical characteristics of fluorometry and absorptiometry in the present approach, in Figure 10, the signal changes of absorbance and fluorescence are plotted as a function of the logarithm of copper ion concentration. Noted that, in general, the changes in absorbance are positive and those of fluorescence are negative as expected. Since **1** absorbs the light at the excitation position of Zntpp, it controls the amount of light available to excite the porphyrin. In the absence of copper ion, **1** hardly absorbs light at 556 nm, the light available to excite Zntpp is thus nearly the same as the initial excitation light. As the concentration of copper ion increases, **1** absorbs more light at 556 nm, so there is less light available to excite the porphyrin, which causes a decrease in the fluorescence emission.

From Figure 10, it is clear that the dynamic range of fluorometry shifts to a low copper ion concentration range with respect to that of absorptiometry. At low concentration of copper ion, there is no real change in the absorbance of **1** while there is clearly a significant decrease in the fluorescence intensity of Zntpp upon increasing copper ion concentration. It probably can be even improved by further optimizing the amount ratio of the absorber and the fluorophore. The improvement in the limit of detection and dynamic response range caused by IFEs can be explained by the intrinsic relationship between fluorescence and absorbance; i.e., the changes in the absorption of the absorber translate into exponential changes in fluorescence. In addition, we attribute the enhanced sensitivity of our sensor to the large extinction coef-

ficient of the copper complex of **1** as well as the relative excess of absorber over the fluorophore. As a result, even small changes in the copper ion concentration cause a substantial change in the effective intensity of excitation light beam of the fluorophore, and thus in its fluorescence emission intensity.

CONCLUSION

The work described here demonstrates for the first time the feasibility of exploiting the absorption-based spiropyran derivative as a fluorescent sensor approach to detect metal ion via the inner filter effect. Compared with classical fluorescent probes for Cu²⁺ detection in which the donor atoms are part of the fluorophore π -system, the spatial separation of chelating group and fluorophore offers considerable flexibility in design. The selectivity is governed by the binding affinity of the absorber with the metal ion, while the sensitivity and dynamic working range of the fluorescence response is dependent on the extinction coefficient of the metal complex of the absorber as well as the relative amount of the absorber and fluorophore. The binding of **1** with copper ion presents an excellent selectivity in comparison with several other transition metal ions. Moreover, because the changes in the absorption of the absorber translate into exponential changes in fluorescence, this scheme offers an attractive alternative to absorptiometric as well as fluorometric technique using one single dye with respect to the response sensitivity. The sensing approach presented here seems to be a very flexible and general and can be applied to any absorption-based sensor by selecting a suitable fluorophore.

ACKNOWLEDGMENT

Financial support from the National Science Foundation of China (Grant 20475005) is gratefully acknowledged.

SUPPORTING INFORMATION AVAILABLE

Absorption and fluorescence response curves of **1** + Zntpp to metal ions, fluorescence decay curves, and HNMR spectra of **4**, **5**, **7**, and **1**. This material is available free of charge via the Internet at <http://pubs.acs.org>.

Received for review June 8, 2005. Accepted September 5, 2005.

AC051010R